NOVA SCHOOL OF SCIENCE & TECHNOLOGY

DEPARTAMENT OF MATERIAL SCIENCE

Vitor Manuel Vieira Nunes

BSc in Materials Engineering

DEVELOPMENT OF PAPER-BASED, LASER INDUCED GRAPHENE NONENZYMATIC BIOSENSOR FOR GLUCOSE DETECTION

MASTER IN MATERIALS ENGINEERING

NOVA University Lisbon

September, 2024

DEPARTAMENT OF
MATERIAL SCIENCE

DEVELOPMENT OF PAPER-BASED, LASER-INDUCED GRAPHENE ELETROCHEMICAL BIOSENSORS FOR INSULIN DETECTION

VITOR MANUEL VIEIRA NUNES

BSc in Materials Engineering

Adviser: Dr. Emanuel Carlos
Assistant Researcher, NOVA School of Science and Technology

Co-adviser: Tomás Pinheiro
PhD Student, NOVA School of Science and Technology

Examination Committee:

Chair: Dr. Rita Maria Mourão Salazar Branquinho,
Associate Professor, NOVA School of Science and Technology

Rapporteurs: Dr. Henrique Miguel Martiniano Vazão de Almeida,
Researcher, NOVA School of Science and Technology

Adviser: Dr. Emanuel Carlos,
Assistant Researcher, NOVA School of Science and Technology

MASTER IN MATERIALS ENGINEERING

NOVA University Lisbon
September, 2024

DEVELOPMENT OF PAPER-BASED, LASER INDUCED GRAPHENE NONENZYMATIC BIOSENSOR FOR GLUCOSE DETECTION

ACKNOWLEDGMENTS

Com a entrega desta tese de mestrado dou por concluída a minha longa e trabalhosa estadia na FCT-UNL. Apesar de todas a curvas e contracurvas que encontrei neste percurso sinto-me orgulhoso de ter finalizado esta etapa académica.

Gostaria de em primeiro lugar agradecer ao CENIMAT por esta oportunidade e aos meus orientadores, Emanuel Carlos e Tomás Pinheiro, pela paciência que tiveram ao longo deste processo.

Um agradecimento muito especial a toda minha família. Ao meu irmão, Marcelo Nunes, que apesar de todas as desavenças que tivemos ao longo da nossa vida sempre procurou que eu desse o meu melhor e que nunca desistisse do meu curso por mais complicada e confusa que estivesse a minha situação académica. Ao meu pai, Eduardo Nunes, por ser um exemplo de pessoa a seguir e ser a personificação da palavra "Superação". Apesar de todos os infortúnios que lhe apareceram na vida nunca se rendeu a vitimização. Enfrentou tudo o que tinha pela frente procurando sempre dar exemplo correto aos seus filhos e sempre com um sorriso na cara. E à minha mãe, Águeda Nunes, que devo de chamar de "Super-Mãe". Depois do acidente que o pai teve durante 4 anos foi só tu que aguentaste o barco. Foram 4 anos, de visitas regulares a hospitais e clínicas de reabilitação e a regressar a casa só nós os 3 com a esperança que um dia o nosso pai e teu marido voltasse para casa connosco. Foram 4 anos, sem ajuda nem de amigos nem de familiares em que te dedicaste incansavelmente a criar dois adolescentes revoltados incapazes de entender que infelizmente acidentes acontecem na vida das pessoas. Foram 4 anos, em que fizeste a função de pai e mãe ao mesmo tempo e em que te preocupaste em manter as despesas da casa, do carro, dos hospitais, das clínicas de reabilitação, escolares e pessoais em dia. Mantiveste sempre comida na mesa, coisa que para mim e para o Marcelo nunca faltou, mas para ti mãe não consigo dizer o mesmo. O "Não estou com fome" à hora do jantar que algumas vezes ouvíamos podia ter passado de despercebido no momento, mas mais tarde tive a realização que era um sacrifício da tua parte, que a ideia de veres os teus filhos com fome era uma imagem que nunca querias ver na tua vida nem que isso implicasse que tu própria passasses fome. Mesmo quando o pai voltou a casa a tormenta não passou, foram dois filhos a ir para Lisboa estudar e mais uma vez na estiveste tu na gestão disto tudo. Agora digo com certeza a situação melhorou, o esforço que meteste ao longo

destes anos deu resultado, tens dois filhos com um mestrado e trabalho. E por isso tudo um agradecimento é pouco, mas é o que neste momento consigo dar.

This work was financed by national funds from FCT - Fundação para a Ciência e a Tecnologia, I.P., in the scope of the projects LA/P/0037/2020, UIDP/50025/2020 and

UIDB/50025/2020 of the Associate Laboratory Institute of Nanostructures, Nanomodelling and

Nanofabrication – i3N).

“Eu cheguei onde cheguei porque tudo o que planejei deu errado.” (Rubem Alves).

ABSTRACT

Diabetes mellitus is a persistent metabolic condition that endures throughout an individual's life. Glucose and insulin play a crucial role in the management and regulation of this illness. Frequently, a variety of laboratory tests are utilized for diagnosing and managing diabetes. One of the key diagnostic criteria is the measurement of blood glucose concentration. New studies aim for a non-evasive testing of glucose concentration in other body fluids, specifically sweat. This thesis addresses the issue of expensive glucose sensors by developing a sensor employing nickel nanoparticles (NiNPs), a more affordable transition metal, and investigating a substitute for silver (the metal mainly used in biomedical applications), along with Laser-Induced Graphene (LIG), a fast and straightforward method for generating graphene, on paper substrates. To begin with, the LIG technique provides a quick and easy way to create highly conductive graphitized material, which is valuable for sensing applications, without requiring costly or complicated fabrication methods. Furthermore, it enables the creation of LIG on paper, which is a more eco-friendly, adaptable, cost-effective, and readily available option compared to other frequently utilized materials. A low-cost nickel precursor was chosen for creating NiNPs using a laser, which showed great catalytic activity for glucose oxidation in non-enzymatic detection. Consequently, NiNPs and LIG composites were fabricated together in a single step, enabling the mass production of sensors. The LIG electrode that had obtained the best results had a sheet resistance value of only 18.24 Ohm/sq. The sensor exhibited strong electrochemical performance during cyclic voltammetry assessment. The biosensor showed the ability to detect glucose, but did not reach the required analytical levels within sweat range (20 μM to 1.79 mM), more tests need to be carried out to achieve more favorable results and to find a way to achieve greater deposition of NiNPs on the electrode that will be in contact with glucose.

Keywords: Glucose, paper biosensor, laser-induced graphene, nickel nanoparticles, non-enzymatic, flexible electronics, sustainability.

RESUMO

A diabetes mellitus é uma doença metabólica persistente que se mantém ao longo da vida de um indivíduo. A glucose e a insulina desempenham um papel crucial na gestão e regulação desta doença. Frequentemente, é utilizada uma variedade de testes laboratoriais para diagnosticar e gerir a diabetes. Um dos principais critérios de diagnóstico é a medição da concentração de glucose no sangue. Novos estudos visam um teste não invasivo da concentração de glucose noutros fluidos corporais, especificamente no suor. Esta tese centra-se na resolução do problema dos sensores de glucose dispendiosos através da criação de um sensor utilizando nanopartículas de níquel (NiNPs) e grafeno induzido por laser (LIG) num substrato de papel. Para começar, a técnica LIG proporciona uma forma rápida e fácil de criar material grafitizado altamente condutor, que é valioso para aplicações de deteção, sem exigir métodos de fabrico dispendiosos ou complicados. Além disso, permite a criação de LIG em papel, que é uma opção mais ecológica, adaptável, económica e facilmente disponível, em comparação com outros materiais frequentemente utilizados. Foi escolhido um precursor de níquel de baixo custo para a criação de NiNPs utilizando um laser, que mostrou uma grande atividade catalítica para a oxidação da glucose em deteção não enzimática. Consequentemente, as NiNPs e os compósitos de LIG foram fabricados em conjunto numa única etapa, permitindo a produção em massa de sensores. O elétrodo LIG que obteve os melhores resultados tinha um valor de resistência de folha de apenas 18,24 Ohm/sq. O sensor apresentou um forte desempenho eletroquímico durante a avaliação por voltimetria cíclica. O biossensor mostrou a capacidade de detetar a glucose, mas não atingiu os níveis analíticos necessários dentro da gama de suor (20 µM a 1,79 mM), sendo necessário desenvolver mais ensaios para alcançar resultados mais favoráveis e encontrar uma maneira de conseguir uma maior deposição de NiNPs no eletrodo que estará em contato com a glucose.

Palavras chave: Glucose, biossensor de papel, grafeno induzido por laser, nanopartículas de níquel, não enzimático, eletrónica flexível, sustentabilidade.

CONTENTS

LIST OF FIGURES

List of Tables

ACRONYMS

CE	Counter Electrode.
CO_2	Carbon Dioxide.
CV	Cyclic Voltammetry.
EG	Ethylene glycol.
EDS	Energy Dispersive X-Ray Spectroscopy.
GNs	Graphene Nanosheets.
GO	Graphene Oxide.
LIG	Laser Induced Graphene.
NiNPs	Nickel Nanoparticles.
SEM	Scanning Electron Microscope.
XRD	X-Ray Diffraction.
WE	Working Electrode.

MOTIVATION AND CONTEXT

Impaired insulin secretion can lead to diabetes, renal failure, obesity, and neurological disorders. Insulin is crucial for regulating the levels of glucose in the bloodstream of humans. Hence, early detection with high sensitivity and specificity is crucial for timely diagnosis and treatment of insulin-related conditions.

More precisely, diabetes can manifest in two distinct forms: type 1, characterized by insufficient insulin production from the pancreas, and type 2, linked to the body's inability to effectively utilize insulin due to resistance [1]. The development of diabetes is multifaceted, with factors such as genetics, environment, demographics, and behavior playing a role. All these factors influence insulin, leading to the disruption of blood sugar levels and various harmful consequences on small and large blood vessels, such as heart issues, nerve damage, and vision problems. Therefore, it is essential to regularly monitor glucose levels to effectively manage diabetes.

Various techniques are employed for conducting such measurements, but they tend to be costly and intricate. Therefore, there is an opportunity in this competitive sector to create simple, affordable, and environmentally friendly measurement systems.

The utilization of biosensors has significantly advanced in recent years and can be implemented across a range of samples. Paper, being a material that's easy to obtain and easy to recycle, is currently being utilized in the realm of electrochemistry because of its eco-friendliness, accessibility, and affordability and being used in capacitors and supercapacitors, transistors, batteries, sensors, etc., as cellulose-based substrate [50].

Producing graphene, a natural material with excellent electrical properties, can be complicated and costly. Using lasers to create laser induced graphene solves the problem by allowing the production of graphene through the interaction of a CO_2 laser with a pre-treated paper substrate. This could lead to the creation of a cheaper and eco-friendly option for monitoring glucose levels. This thesis intends to create a low-cost, eco-friendly glucose/insulin sensor that does not require enzymes and can be incorporated into a wearable device for non-invasive detection of glucose/insulin from sweat. The sensor will be created using Laser-Induced Graphene (LIG) and nickel nanoparticles (NiNPs) on paper for detecting glucose/insulin without using enzymes.

1. INTRODUCTION

1.1 Graphene

There is ongoing major interest in carbon nanostructures in various fields, such as sensors, high-speed electronics, and storage applications. Different types of carbon materials, including amorphous carbon, graphite, diamond, carbon nanotubes, and the more recently found graphene [2], come in various forms. The improved quality of graphene-based sensors among these different forms of carbon has sparked interest in these nanostructures. Graphene is described as a single layer of carbon atoms arranged in a benzene-ring formation, with 0.142 nm between them [3], and it has become the top choice for application in pliable and adaptable devices. Graphene has attracted a lot of interest thanks to its outstanding physical characteristics like remarkable strength, lightweight, flexibility, and superior electrical conductivity. Graphene's vast potential has significantly affected various industries, including coatings, flexible devices, and energy storage.

Multiple methods have been documented for producing graphene. There are two types of methods that can be categorized (Figure 1.1).

Bottom-up methods involve heating carbon precursors at high temperatures to produce graphene, such as chemical vapor deposition, epitaxial growth, and laser-induced graphene.

Top-down methods include processes such as exfoliation of stacked graphite layers to create graphene monolayers, arc discharge, unzipping graphene nanotubes, and others.

Both groups have their benefits and difficulties. Overall, top-down methods do not need costly tools, but they do not provide reliable graphene conformity. Even though the creation of high-quality graphene and its growth on specific substrates require advanced infrastructure, bottom-up methods offer convenience for various applications. The most appropriate

synthesis technique for graphene can be chosen based on its intended final use, in order to optimize its advantages.

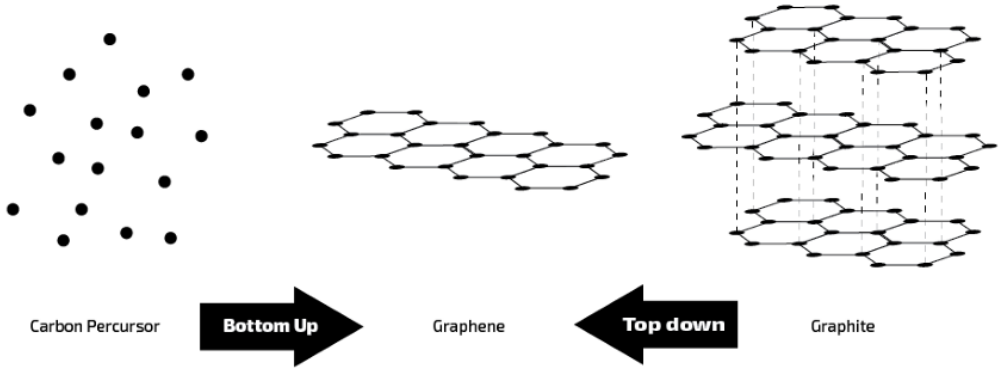

Figure 1.1 — Schematic of different graphene synthesis methods (retrieved from [19]).

1.2 Laser Induced Graphene (LIG)

Given its exceptional physical and chemical characteristics, graphene is utilized in various fields such as electronics and catalysis. Comprised of a single layer of carbon atoms in a hexagonal structure, graphene possesses remarkable electronic transport properties, including high carrier saturation velocity, excellent carrier mobility, and high Fermi velocity. Consequently, it is extensively employed in various forms for biosensor applications.

One of these techniques, known as Laser induced Graphene (LIG), has been utilized for creating multiple graphene electrodes. The quick and uncomplicated synthesis using LIG has resulted in the creation of various laser engraved graphene electrodes, including gas sensors [6], pressure sensors [7], and glucose sensors [8, 9, 10]. LIG is a method that produces extremely conductive graphitic carbon designs using Direct Laser Writing. By using a CO_2 laser source, it is easy to create structures with precise control of patterning and high resolution by exposing a polymer surface to radiation. The high temperatures induced by the laser irradiation lead to bond breaking in the substrate, resulting in the re-organization of carbon bonds into graphene and graphitic structures. Studying the velocity and strength of the laser beam is essential for creating LIG [51].

Furthermore, direct laser writing and resulting LIG is an appropriate method for mass production in ambient conditions as it offers low cost, excellent electron transfer, and a large specific surface area in a quick and binder-free fabrication process [11].

In contrast to alternative methods like laser-reduced graphene, which uses lasers to reduce graphene oxide films, LIG offers a cost-effective and simplified process by eliminating the need for graphene oxide (GO) precursors. This porous graphene-like material can be easily created by directing a strong CO_2 laser onto commercial polyimide foil in ambient conditions.

Pinheiro et al. 2021 utilized LIG in their study to create amperometric, enzymatic glucose biosensors on paper, resulting in the development of a multilayered graphenic material. Characterization and production were conducted on coplanar systems with three electrodes (working, counter, and reference), resulting in the observation of high current Faradaic oxidation and reduction peaks on LIG-based surfaces, indicating a large electrochemical active area [17].

Paper-based electrochemical analytical devices are also employed in the detection of various substances such as dopamine, uric acid, and ascorbic acid [19][20][21].

1.3 Electrochemical Biosensors (LIG Biosensors)

An electrochemical biosensor is a biosensor where its electrode is altered chemically, having an electrochemical transducer as a result [8]. An electrical signal is generated by the biological sensing element within the sensor when it interacts with the analyte, leading to a signal that correlates with the analyte's concentration [22].

In the past decade, there has been significant advancement in electrochemical biosensors, making them the most popular and extensively studied method for wearable glucose monitoring today. Electrochemical sensing offers promise for detecting glucose due to its rapid response, high sensitivity, and selectivity [23]. Hence, electrochemical biosensors are currently dominating the glucose sensor market. These sensors incorporate electrodes that can measure electric properties produced by reduction and oxidation reactions.

Electrochemical sensors' architecture is usually composed of three different electrodes that form the electrochemical cell (shown in Figure 1.2):

- The Working Electrode (WE): the sensor's most crucial element is where the reaction, oxidation, or reduction of the target analyte takes place. The determination of the desired electrical characteristic is greatly impacted by the working electrode as it is where the sensing material is constructed [24]. Choosing the appropriate WE material is essential in achieving

accurate measurements as it needs to facilitate effective electron transfer among the chemical species participating in the reaction [25].

- The Reference Electrode (RE): possesses a consistent and well-known electrochemical potential. This electrode enables a constant potential, so any alteration in the cell relates to the WE [26]. The Ag/AgCl reference electrode is the most utilized in electrochemical sensing for aqueous solutions because it provides stable potentials that remain constant regardless of time or temperature fluctuations [24].

- The Counter Electrode (CE) is regarded as an auxiliary electrode and is utilized to finalize the electrical circuit. This electrode does not participate in the chemical reaction; its sole function is to facilitate the flow of current between the WE and the CE [27]. In order to prevent restrictions in the reaction kinetics, the electrode's surface area should be significantly greater than that of the working electrode [28]

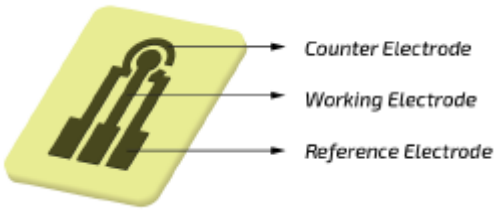

Figure 1.2 — Representation of a three-electrode electrochemical sensor (retrieved from [19]).

Electrochemical sensors can be divided into different approaches to measuring analyte concentrations. Voltammetry, amperometry, potenciometry and impedance spectroscopy are the four main types of electrochemical methods of detection. This thesis will use voltammetry techniques to characterize and optimize the sensor performance and try to develop an amperometric sensor for glucose detection. Voltammetry is based on the measurement of a current response as a function of varying applied potentials between the WE and RE [29]. The voltammogram, which is the resulting plot of current vs potential, provides quantitative and qualitative information about the species involved in the redox reaction [30]. This category groups several voltammetric methods that, using a potentiostat, apply specific voltage profiles to the WE. In this thesis we are focusing more on Cyclic Voltammetry (CV) [24].

An amperometric measure differs from the voltammetric one since the applied potential is fixed. It works by measuring the generated current from the targeted analyte catalysis in a chemical reaction, as a function of time. Through the application of a constant potential

between the WE and the RE, the produced electrons migrate between the WE to the CE and electrical current can be measured. The resulting electrical current directly derives from the electron transfer rate, and it is proportional to the analyte concentration [31]. Next, a general insight of the working principles of CV is presented, since this technique will be extensively used in this work.

1.4 Nickel Nanoparticles

The attention is now shifting from enzyme-based glucose detection methods to non-enzymatic options. Metallic nanoparticles and their oxides act as active substances with the ability to oxidize glucose directly on the electrode's surface. The interest in using nickel nanoparticles (NiNPs) as a modification material is due to its affordability compared to Ag, Pd, or Pt, while still sharing some characteristics with noble metal nanoparticles. At the same time, Ni-based nanomaterials show exceptional catalytic abilities for insulin due to the redox reaction of $Ni(OH)_2$/NiOOH at the electrode surface in an alkaline environment. Various methods have been used to attach NiNPs onto electrode surfaces including electrochemical deposition, seed-mediated growth, magnetron co-sputtering deposition, and drop casting [32]. The size and shape of NiNPs can be greatly influenced by their synthesis method and precursors, which in turn can affect their catalytic activity [35].

2. EXPERIMENT METHODOLOGY

2.1 Fabrication of LIG Sensors

2.1.1 Fire Retarding Treatment of the Paper Substract

Sheets of Whatman chromatography paper grade 1 were trimmed into A6 shape before being placed in a 0.1 M sodium tetraborate decahydrate (1303-96-4, Sigma-Aldrich, 99.5%) + 40mM nickel nitrate solution (13478-00-7, Sigma-Aldrich, 98.5%) for 20 minutes (10 minutes each side) with constant stirring. The leftover mixture was gathered, and each piece was allowed to air dry individually (Initially dried in a vertical position and later dried horizontally. This was because there was a higher concentration of nickel in the bottom of the paper when dried vertically, and it was desired to have nickel evenly distributed throughout the paper.) till the piece of paper was fully dried.

Previous research has indicated that the number of wax layers affects the sheet resistance of LIG electrodes, so the initial test samples were split into two groups: one containing 4 layers of wax and the other containing 5 layers of wax. The wax used was a yellow wax (Xerox Solid Ink) printed with Xerox ColorQube printer. Between each print the wax was liquified and spread to the opposite side of the paper using a heating plate set at 120°C.

2.1.2 Assembling of the sensor

Laser engraving - The eletrode design was engraved with a commercial CO_2 laser (Universal Laser System VLS3.50) connected to a nitrogen hose (open while in use) with maximum power value (50 W) and maximum speed (1.25 m/s) , using power (P) ranging from 6% to 8% and speed (S) ranging from 5% to 12% for various samples, with the paper placed on a glass surface for the engraving process.

Encapsulation and painting - The outcome was that the strips were sealed in A6 laminating pouches (Staples Europe BV., The Netherlands) using heat treatment (Quigg, Essen, Germany). The sensor's contacts were coated with AG-510 (Conductive Compounds, Inc., Hudson, NH) silver ink and the reference electrode with Ag/AgCl ink (AGCL-675, Conductive Compounds, Inc., Hudson, NH). Afterwards, the ink was heated at 50 °C on a hot plate for 1 hour till fully annealed.

2.2 Drop Casting

This thesis utilized the drop cast method to provide an alternative approach for incorporating Nickel precursor into LIG electrodes. The paper substrate underwent the same chemical treatment with 0.1M sodium tetraborate decahydrate (only) and followed the same procedure. Initially, a single layer of yellow wax with a unique design is applied, featuring ponds for casting drops. Afterwards, the wax is melted and spread under the same conditions as previously mentioned. The ratio used for drop casting was 0.5 µL/mm^2 for a 16 mm^2 square area. Several options were employed in this procedure to replace nickel nitrate precursor: nickel acetate (6018-89-9, Sigma-Aldrich 99.0%), nickel chloride (7718-54-9, Sigma-Aldrich, 98%), nickel sulfate (10101-97-0, Sigma-Aldrich, 98%) and a combination of nickel nitrate with a 10% (v/v) ratio of ethylene glycol (107-21-1, Sigma-Aldrich, anhydrous, 99.8%) to aid in dilution and prevent suspension formation.

2.3 Electrochemical Characterization

CV and chronoamperometry were used to assess the functionality of glucose sensing without the use of enzymes.

CV experiments were carried out at a scan speed of 10 mV s^{-1} and a potential range from -2 to +2 V to study nickel oxidation states transitions. The redox probe $[Fe(CN)_6]^{3-/4-}$ was utilized in all electrochemical assays conducted with a 5 M ferri/ferrocyanide solution (14038-43-8, Sigma Aldrich, 100%). prepared in the supporting electrolyte, at multiple scan rates of 10, 30, 50, 70, 90, 110, 120, 130 or 150 mV s^{-1}, for 6 cycles each. 60 µL of this mixture were pipetted to the electrode working area delimited by the plastic mask. For the CV essays carried on NiNPs-LIG based sensors, this window was adjusted to –0.4 to +0.7 V.

The chronoamperometric technique was chosen to track current changes when glucose was added. In discrete measurements, a certain amount of glucose concentration was introduced into the beaker, and chronoamperometry was performed.

The sensor was secured using a retort stand and a three-claw clamp, with connections to the potentiostat made through crocodile tips on both electrodes (figure A1). A solution with a glucose (50-99-7, Sigma-Aldrich, 99,5%) concentration of 100 mM was mixed into a 50 mL beaker with 0.1 M NaOH (1310-73-2, Sigma-Aldrich, 98%) as the supporting electrolyte and a magnetic stirrer. The beaker was positioned onto a magnetic stir plate and all tests were carried out with the stirring speed set to 180 rpm.

After a 300 s duration, allowing sufficient time for the current to reach a stable state the input of glucose starts. This procedure was conducted with varying levels of glucose. During ongoing monitoring, each glucose addition was consistently separated by 100 seconds. 100 µL of the sample in the beaker is removed and the same volume of the glucose solution is added very quickly back in. This method made sure the beaker's content would never touch the sensor's electrical contacts by keeping its volume under 50 mL. Various applied potentials (0.4, 0.5, and 0.6 V) were experimented with to determine the optimal electrochemical response and identify the most appropriate standard potential.

2.4 Characterization Equipment

Potentiostat – PalmSens4 potentiostat was used for electrochemical characterization by means of cyclic voltammetry and chronoamperometry. This equipment was used in several tests using various electrolytes such as solutions 5 M ferri/ferrocyanide, $[Fe(CN)_6]^{3-/4-}$ as the redox probe and glucose solutions.

Hall Effect – In order to determine which, set of laser conditions was more appropriate to use (Laser speed and power), the sheet resistance was measured using the Accent HL5500PC Hall Effect Measurement System.

Scanning Electronic Microscope (SEM) - Hitachi TM 3030Plus Tabletop Microscope was used in Whatman chromatography paper, LIG samples and LIG with NiNP samples with the objective of characterize and analyze its surface (morphology, existence of NiNP in the sample and composition).

Raman Spectroscopy – Chemical characterization of LIG samples was also determined by Raman spectroscopy spectra. The equipment used was the inVia confocal Raman microscope.

Raman spectras were obtained using a laser with 532 nm of wavelength, for 10 seconds, 3 cycles with a 10 % power.

X-Ray Diffraction (XRD) - A non-invasive method that offers in-depth data on the crystal structure of materials was utilized to generate diffractograms for NiNPs-LIG samples to confirm the presence of NiNPs in the LIG samples. The PANalytical XPert PRO MRD equipment was utilized.

3.

RESULTS AND DISCUSSION

3.1 Biosensor Design and Electrochemical Fundamentals

According to the criteria necessary for a biosensor to be effective and with reference to earlier studies, the created sensor was engineered to fulfill all the criteria, demonstrating excellent specificity, reproducibility, stability, and sensitivity, in addition to being safe, economical, and capable of conducting real-time analysis. The image displayed below illustrates the sensor that was created (figure 3.1).

This design features a round working electrode measuring 4 mm in diameter and a curved reference and counter electrode. Silver ink was used to paint the electrical contacts since this pattern is frequently utilized in electrochemical sensors [18].

The round shape of the working electrode (WE) was selected instead of a rectangular shape because tests in CV showed that this design had a more favorable electrochemical response and is easier to carry electrode modifications by drop-casting methods [18] [36] [37].

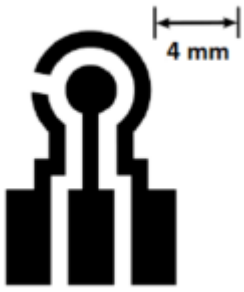

Figure 3.1 — Schematic of a Three-electrode design for the detection of glucose used in this thesis.

3.2 LIG Laser Parameters (Power and Speed) Optimization for the Different Paper Treatments

The power and speed of the laser has a huge impact on the quality of the produced graphene. In general, high power percentage leads to thicker graphene which therefore increases conductivity. However, high percentage of power coupled with low percentage of speed will result in the burning of the substrate, while high percentage of speed and low percentage of power will not convert the paper into good quality LIG. Therefore, it is necessary to find a good relation between these two parameters with the purpose finding the ideal condition for LIG formation.

With that in mind, a matrix of laser Induced graphene was produced with speed percentage from 5% to 12% and power increasing from 6% to 9% and for 1 and 2 passings of the laser, as shown in Figure 3.2 a). These conditions were chosen based on previous works [17][18][19], so validation was required. With that in mind, it was decided that the ideal combination of power/speed would be such that the power percentage should be lower or the same as the speed percentage, since for those values the produced graphene presented clearer patterns, and it is usually the conditions used in other works. Also, the quantity of graphene present in the sample should be such that it could not be easily removed when used for glucose measuring.

In order to determine which condition was more fitting to be applied in the sensor, sheet resistance was used as an eliminating factor, so the combinations that had less sheet resistance were selected (Figure 3.2 b).

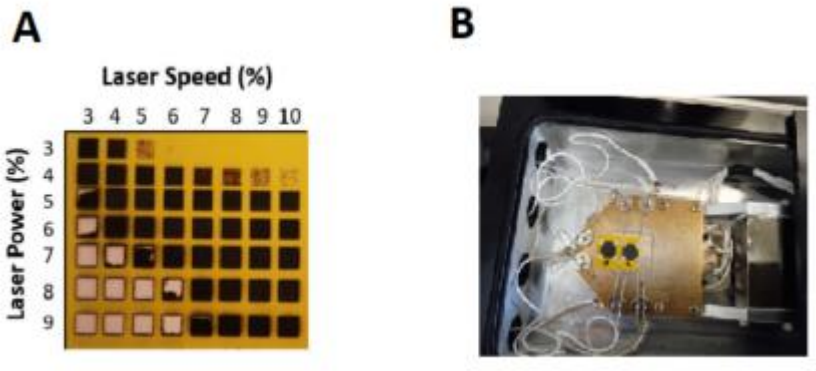

Figure 3.2 — (A) Laser-engraved matrix of laser power vs speed on paper substrate, (B) LIG samples on Hall Effect for sheet resistance measurement

3.2.1 Samples with 0.1 M sodium tetraborate decahydrate+ 40mM nickel nitrate

For the samples made with the chemical treatment of a 0.1 M sodium tetraborate decahydrate+ 40mM nickel nitrate (with 4 and 5 layers of wax) the laser speed conditions for the following shown in figure 3.3.

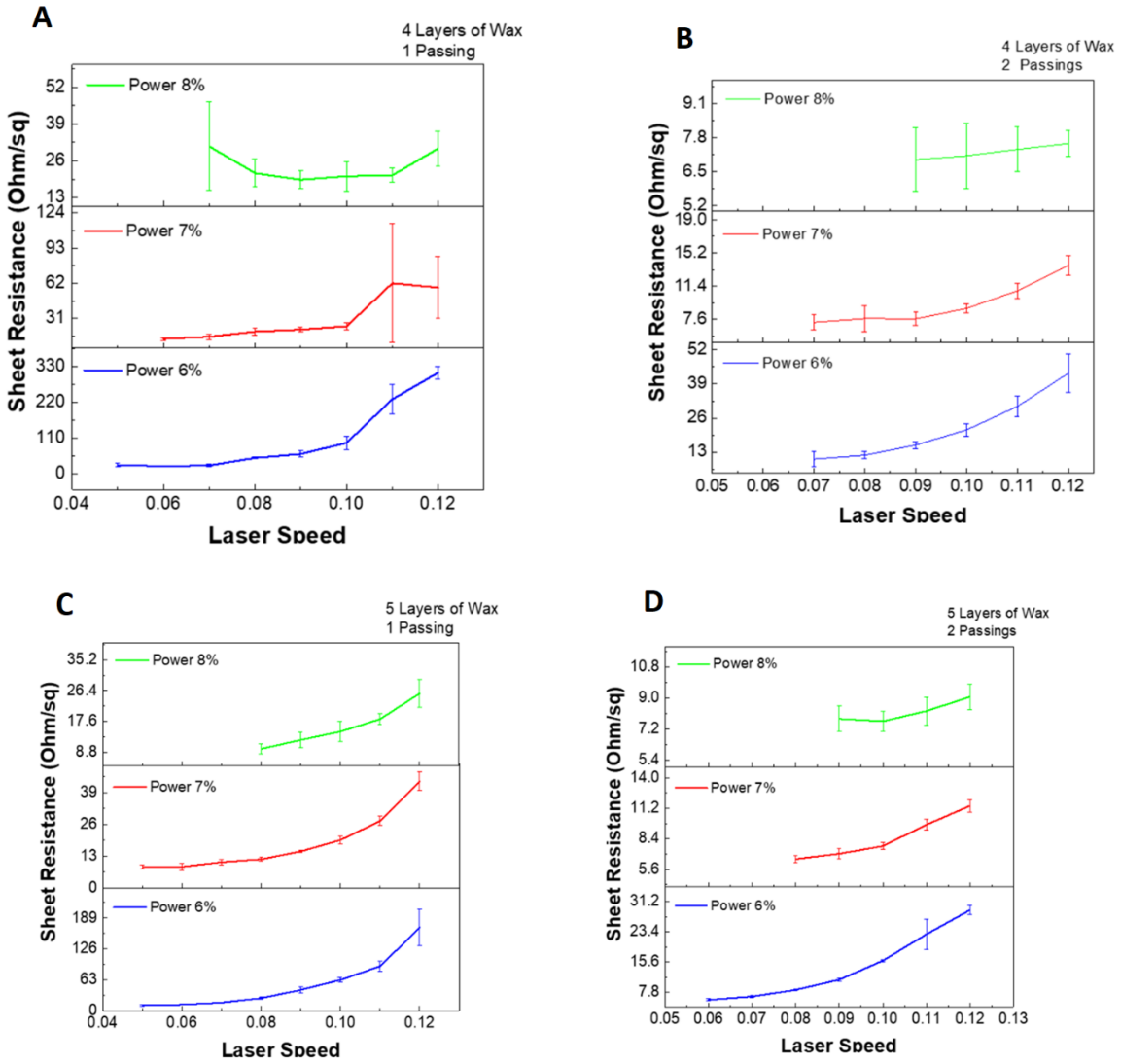

Figure 3.3 — Correlation between different laser speeds and powers and sheet resistance (Ohm/sq) for: (A) 4 Layers 2 Passings, (B) 4 Layers 2 Passings, (C) 5 Layers 1 Passing, (D) 5 Layers 2 Passings.

For 5 layers of wax 1 Passing:

-P6 were chosen following speeds: S6, S7, S9.

-P7 were chosen following speeds: S8, S9, S10.

-P8 were chosen following speeds: S9, S10, S11.

Even though figure 3.3 indicates that lower laser speed results in lower sheet resistance at the chosen Power and Speed settings, higher speed values were chosen because, as later illustrated with SEM images, the longer laser contact time with the chemically treated sample could lead to ablation and potential removal of NiNPs from the sample where LIG is created, thus ruling out two-pass samples that being said, the samples with 4 layers of wax and one laser pass were excluded due to the higher sheet resistance values compared to those with 5 layers of wax and one laser pass, as depicted in figure 3.3. After conducting all the tests and evaluating the corresponding outcomes (to be described in more detail later), the chosen specification for creating the glucose testing electrode was as follows: 5 coats of wax, a single laser passing and P8S11. All sheet resistances values of the chosen conditions are compiled on table A1.

3.2.2 Drop Cast Samples with Nickel Nitrate and Other Nickel Precursors

Seeing that the solution used in the first chemical treatment was saturated with solute (nickel nitrate), this raised the question of whether this nickel precursor should be impregnated in the paper matrix, since the solution being saturated, the precipitate would only be placed on the surface of the paper at the risk of being removed during the wax printing process.
We therefore looked for an alternative way of depositing the NiNP in the paper matrix to obtain a LIG+NiNP composite. Ethylene glycol (EG) (droplet stabilizer) 10% (v/v) was used with nickel nitrate (concentration 40mM) to prevent further solute precipitation since EG serves as a co-solvent to stabilize droplet formation, acting as a gelling agent through the formation of an organic ester. This leads to the creation of a uniform network with metal ions [45][46]. Also, other nickel precursors (with also 40mM concentration) were used to find an alternative to nickel nitrate (figure 3.4).

Figure 3.4 — Different nickel precursors used with the drop cast technique (nickel acetate, nickel sulfate and nickel chloride). All samples present 0.5 µl/mm^2 ratio.

The mixture of 0.1 M sodium tetraborate decahydrate and 40mM nickel nitrate with 10% (v/v) EG produced consistent and reproducible results, as seen in the low standard deviation of the values in figure 3.5. This effect was not observed with other nickel precursors, suggesting that EG effectively homogenized and concentrated the solution in the targeted area. Both nickel chloride and nickel acetate yielded promising findings regarding sheet resistance, however, they displayed a high standard deviation, suggesting challenges in reproducibility and consistency. This occurred as a result of the laser burning numerous samples during the LIG manufacturing process. Although the solution was homogenized and there was no precipitate, more samples appeared burnt after the laser pass (nickel sulfate were burned for all the laser powers and speeds combinations). This leads us to believe that adding another solution to the already dried and chemically treated paper could cause the sodium tetraborate to dissolve again, nullifying the first chemical treatment and leaving the paper more susceptible to being burnt by the laser beam. The samples made with these precursors and the mixture with ethylene glycol also showed higher sheet resistance values than the samples with the initial treatment and were therefore not used to make the electrode for measuring glucose.

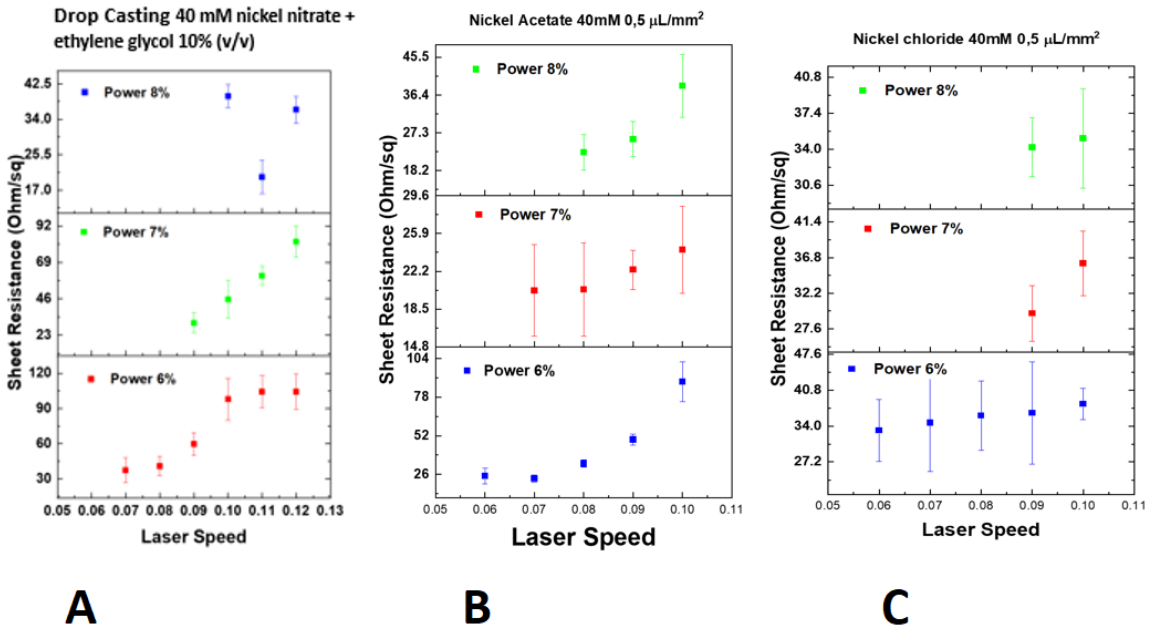

Figure 3.5 — Correlation between different laser speeds and powers and sheet resistance (Ohm/sq) of the different laser conditions for different nickel precursors with 5 Layers of wax and the same 0.5 µl/mm^2 ratio: (A) Nickel Nitrate + Ethylene Glycol (10% v/v), (B) 4 Nickel Acetate, (C) Nickel Chloride.

3.3 Chemical Characterization

3.3.1 Raman Spectroscopy Analysis

Raman spectroscopy tests confirmed that the paper treated with the laser had successfully converted to graphene. This method relies on the dispersion of radiation that occurs in a specific material under monochromatic light exposure. The various frequencies of scattered radiation reveal the molecular vibrations and structural characteristics of a material [38]. Therefore, by utilizing this method, we can conveniently detect the existence of graphene in the specimen through comparison with additional graphene data. Spectra of the samples tested in this work are shown in Figure 3.6 under different laser conditions.

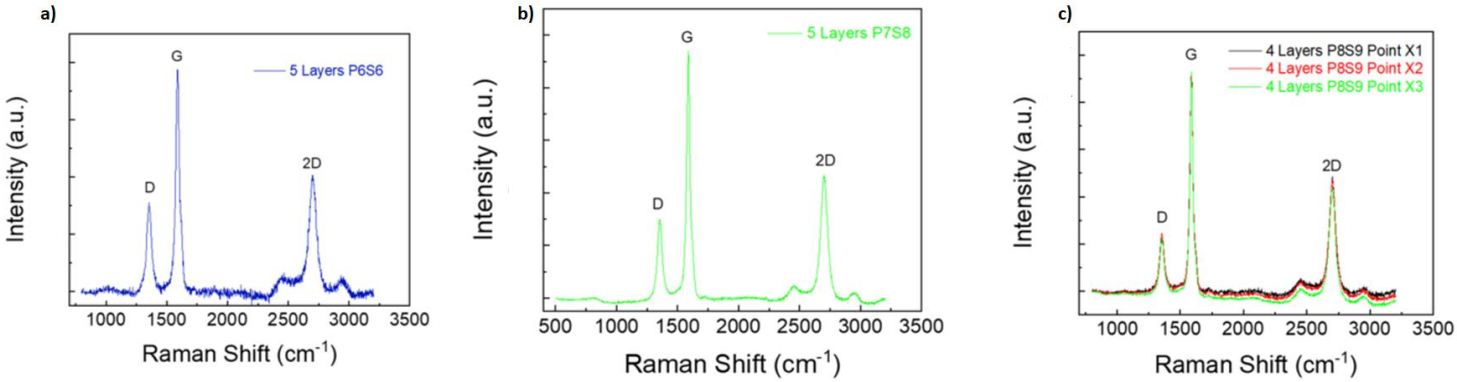

Figure 3.6 — Raman spectrums of the LIG produced using the following laser speed conditions: a) P6S6, b) P7S8 and c) P8S9. To analyze the carbon structures, present in the samples.

The spectrums exhibited three primary peaks: D, G, and 2D, with Raman shift values of 1343, 1569, and 2672 cm^{-1}, respectively. We can infer that the samples exhibit a structure consisting of laser induced graphene, as the Raman shift values for the specified peaks closely match those of other LIG samples [39][40].

These peaks are a common feature in carbon-based formations, yet they embody distinct elements.

The D peak is employed for detecting flaws in disordered parts of the graphene as it indicates imperfections in the hexagonal carbon atom sheets sp2 carbon hybridization. Conversely, the G band is associated with the stretching of sp2 atoms in graphene and first-order inelastic processes, while the 2D peak is connected to second-order processes [17].

The important parameters can also be determined by analyzing the peak intensity ratios in the Raman spectrum. ID/IG provides data on the quality of graphitization, whereas I2D/IG evaluates the alignment of the graphene layers. An I2D/IG value greater than 2 is commonly seen in monolayer graphene, but in the samples examined, the I2D/IG value was approximately 0.55, indicating the multilayered structure of the created LIG. In contrast, ID/IG had a value of approximately 0.67, suggesting a moderate amount of faulty graphitic structures. [41].

3.3.2 XRD Analysis

The crystalline structures of NiNPs-LIG composites were tested using XRD for structural characterization. To gain a deeper insight into how the laser affects the creation of nanoparticles, samples of paper treated with nickel nitrate solution and subjected to a laser pass were examined.

The standard positions (figure 3.7) of the diffraction peaks of Nickel can be observed in the three diffraction peaks on figure TYR, located approximately at 2Θ ≈ 45, 52, and 77, corresponding to the crystal planes (1 1 1), (2 0 0), and (2 2 0) of face-centered cubic (FCC) Ni (JCPDS, file No. 04-0850) [35] [47].

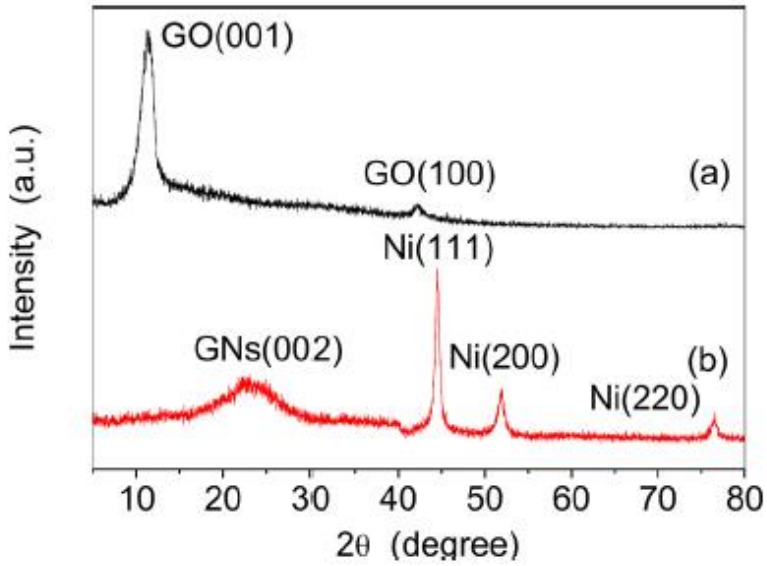

Figure 3.7 —XRD patterns of the as-prepared GO (a) and NiNPs/GNs composites (b). Retrieved from [35].

As can be seen from the results obtained from the samples present in the figure 3.8, it was not possible to verify the crystallographic state of Nickel. In order to ensure the existence and presence of nickel nanoparticles, it was necessary to make SEM analysis as could be seen in the next subsection.

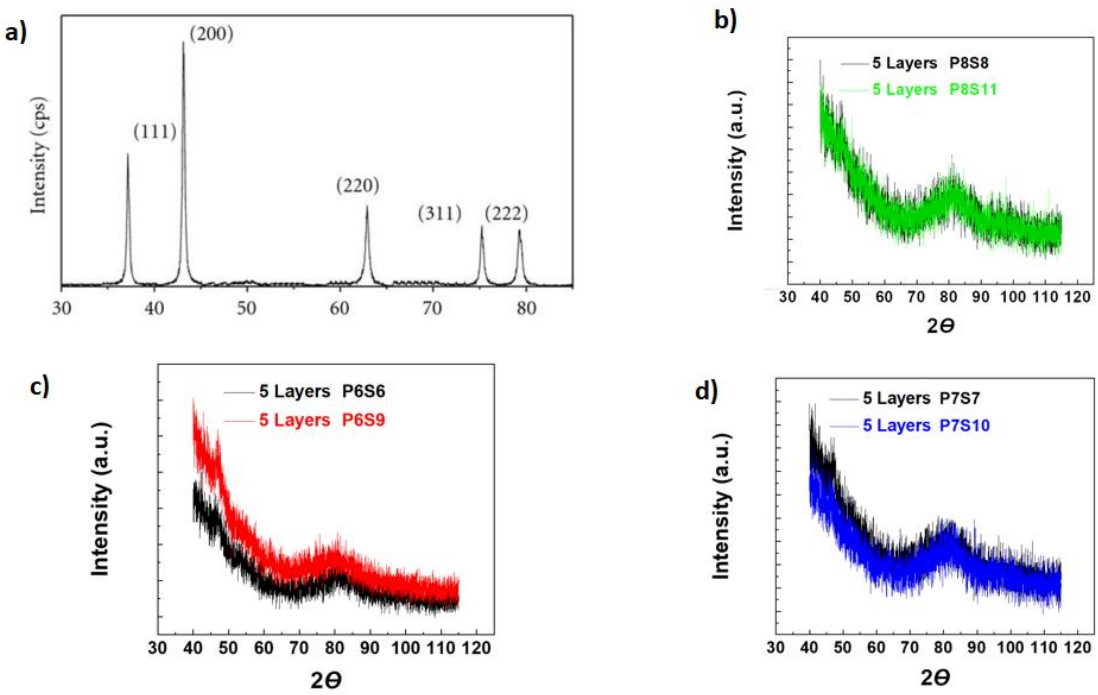

Figure 3.8 —a) Standard XRD of NiO nanoparticles. XRD patterns of the LIG/NiNPs samples produced with 5 layers of wax. b) Samples with the following laser conditions P8S8 and P8S11, c) Samples with the following laser conditions P6S6 and P6S9, d) Samples with the following laser conditions P7S7 and P7S10.

3.4 Morphological Characterization (SEM)

SEM uses an electron beam to scan the sample surface, where information about the probe structure is determined through the production and detection of secondary and backscattered electrons resulting from this interaction. This is a valuable technique for characterizing a sample, as it can reveal details about the material's chemical composition, surface topography, and geometric structure [42].

In this study, scanning electron microscopy was used to initially examine the LIG structures on the paper surface. As the XRD results were inconclusive regarding the existence of NiNPs in their crystalline form, the chosen samples were further analyzed to determine if NiNPs were present on the LIG. In figure 3.9, bright droplets of NiNPs can be observed on the LIG fibers, reflecting the electron beam. The images show the uneven distribution of nickel nanoparticles on the fibers, with different sizes. Although this type of bright droplet appears in

various samples with different laser conditions, the P8S11 exhibited the highest dispersion of nickel droplets in the LIG matrix and had the biggest droplets, as depicted in figure 3.9 a). EDS, shown in figure 3.9 c2), was utilized to confirm that the various droplets present on the LIG fibers consist of nickel.

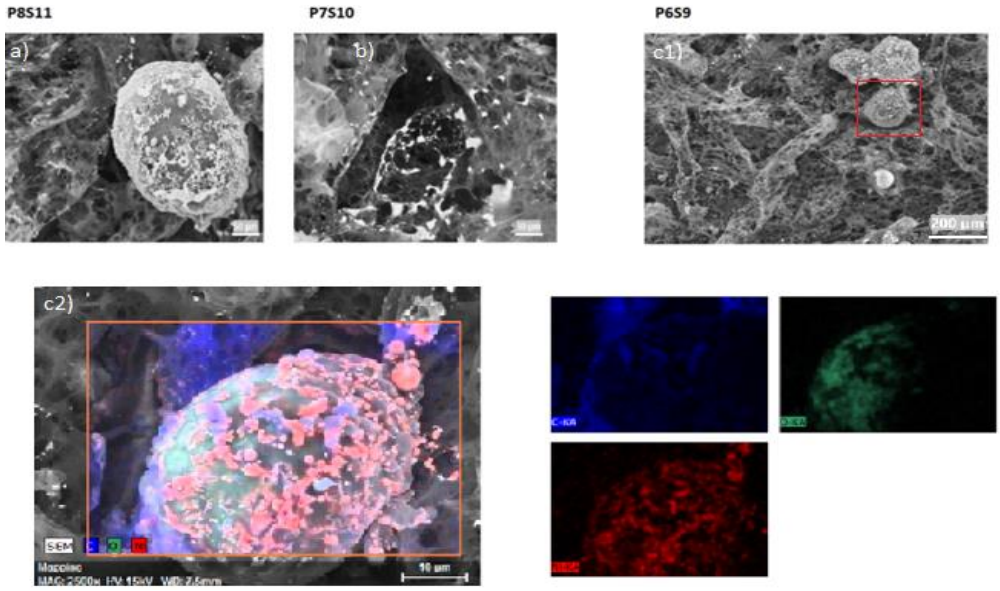

Figure 3.9 —SEM images of LIG/NiNPs for different laser conditions at 800x: a) P8S11, b) P7S10, c1) P6S9, c2) P6S9 sample EDS in a droplet of nickel

As represented on the figure 3.10, it is very noticeable the differences in the structure between LIG and paper, as represented on their interface (brown/yellow interface in figure 3.10). It is visible that, upon lasering, the paper fibers became less smooth and more irregular, which increases the porosity of the surface.

Since the images of the LIG structure were taken on the pattern of the biosensor, it becomes clear that the pattern is indeed made of LIG, however, the increase of porosity of the sample can be detrimental for the electrical performance of the sensor, since capillarity will increase and subsequently solutions drop-casted on LIG surface may invade the substrate and consequently the contacts, which can provoke the malfunction of the sensor [18].

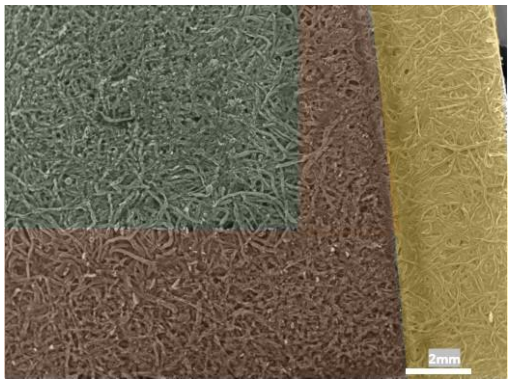

Figure 3.10 —SEM images of a LIG/NiNPs sample where you can see the different areas where they meet: simple paper fibers (yellow), formed LIG (brown), area where there is greater concentration of NiNPs (green).

3.5 Electrochemical Characterization and Glucose Testing

3.5.1 Cyclic Voltammetry (CV)

In cyclic voltammetry, an initial potential, which will be scanned, is applied to an electrochemical cell. This potential of the working electrode vs the reference electrode is controlled by a potentiostat [43] and ranges from two preselected potentials at a certain scan rate, which determines the time scale of the experiment [44]. So, this scan rate continues until the limit potential is reached where it reverses direction, returning to the initial potential [43] and a plot of the current vs potential is obtained by means of the current flow in the cell.

To test our samples, we used as an electrolyte a solution of 5 M ferrocyanide, $[Fe(CN)_6]^{3-/4-}$ as a redox probe, as used in different previous works under the same working conditions. [17] [19]

Figure 3.11 (a) represents a typical CV curve, as well as the meaning of each peak where the peak with positive current is related to an oxidation reaction and the negative peak to a reduction reaction [58]. This is a representation of cyclic voltammetry and its similar to the curve presented on Figure 3.12, where the sensor responds to certain potentials within the determined potential window by oxidation or reduction processes.

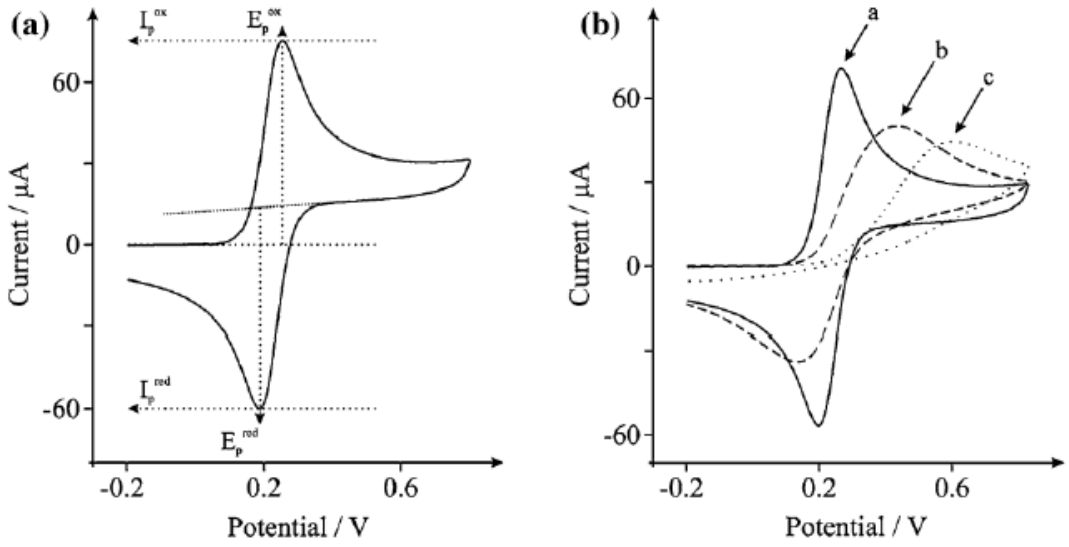

Figure 3.11 —(a) Typical cyclic voltammogram depicting the peak position EP and peak height IP. (b) Cyclic voltammograms for reversible (a), quasi-reversible (b) and irreversible (c) electron transfer. Retrieved from [52].

On the other hand, Figure 3.11 (b) shows three different electrochemical systems: reversible, quasi-reversible and irreversible. The differences between them are related to the velocity of the electrode kinetics and the mass transfer rate, where reversible systems present higher values for this metrics than quasi-reversible which, however, present higher values than the irreversible system. Comparing the shape of these curves with the ones presented on Figure 3.12, we can assume that our sensor responds like a quasi-reversible system.

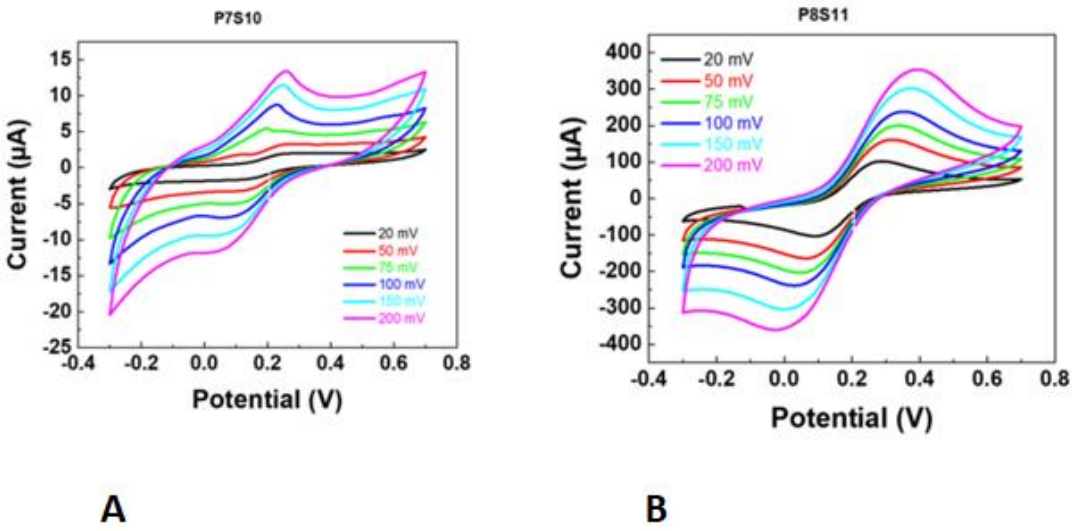

Figure 3.12 —Cyclic voltammetry against ferri-ferrocyanide redox probes of LIG/NiNPs biosensors with the following laser conditions: A) P7S10, B) P8S1.

Examining the graphs from Figure 3.12, taken from the biosensors in development with different combinations of power and speed, it is shown a consistent variation in current alongside the rise in scan rate, along with a minor change in potential values. This shows that the biosensors design is suitable for electrochemistry and can be utilized in the upcoming experiments and P8S11 shows a CV graph very similar to the standard graph showing us this type of electrode formation conditions will be used to test glucose.

3.5.2 Continuous Amperometry and Glucose Testing.

After selecting the conditions with the best results, the substrate's chemical treatment, laser beam conditions, sheet resistance and cyclic voltammetry (P8S11) were selected. The electrode was tested with glucose.

Wang, Bo, et al. (2014) examined how well graphene nanosheets (GNs), NiNPs, and NiNPs/GNs can catalyze reactions using cyclic voltammetry (CV) and continuous amperometry in 0.1 M NaOH solution without and with 1 mM glucose, all at a scan rate of 50 mV s-1 (consistent with another research in the thesis). According to the literature sources [35], the way NiNPs/GNs respond to the electrochemical oxidation of glucose can be described simply as:

$$Ni(OH)_2 + H^- \rightarrow NiO(OH) + H_2O + e^- \quad (3.1)$$

$$NiOH(OH) + Glucose \rightarrow Ni(OH)_2 + Glucolactone \quad (3.2)$$

Figure 3.13 (A and B) displays the amperometric reactions of the NiNPs/GNs for nonenzymatic glucose detection as more glucose is added every 50 seconds in 0.1 M NaOH at +0.5 V.

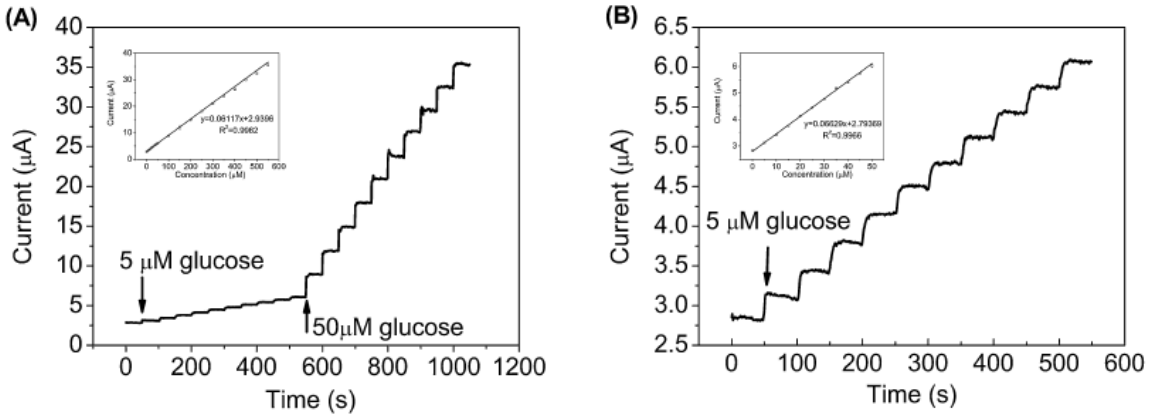

Figure 3.13 —The expected amperometric response of the NiNPs with successive addition of glucose from: (A) 5–550 mM, and (B) 5–50 mM in 0.1 M NaOH solution with stirring at an applied potential of +0.5 V, and the linear relationship between the catalytic current and glucose concentration were inset, respectively. Retrieved from [35].

An abrupt rise in the current reactions occurred with every glucose solution added, reaching a consistent current level in just 3 seconds, demonstrating the high sensitivity and quick response of the NiNPs/GNs. This may be due to the enhanced electron transfer and strong catalytic efficiency made possible by the joint structure of Ni nanoparticles and graphene. The findings suggested that NiNPs/GNs have the potential for accurate and precise glucose detection. Therefore, this study established a benchmark for evaluating the amperometric examination of our samples, as the desired outcome in this research is to observe the "ladder effect" upon the addition of glucose.

At first, we replicated the procedures from past research on glucose detection with non-enzymatic paper biosensors [19][35]. We allowed 300 seconds for the biosensor to stabilize in a NaOH solution, then added 50 µL of glucose solution every 100 seconds with glucose solutions of different concentrations as outlined in the experimental protocol. An immediate response was anticipated, and the "ladder effect" was expected to be confirmed, as depicted in figure 3.13, but this did not happen.

To confirm that the manufactured biosensor would detect glucose, we used a solution of glucose with a concentration of 100 mM and the volume pipetted was increased to 100 µL for the same duration (both stabilization and waiting time between pipetting). In accordance with figure 3.14, a slight step response of the biosensor to the introduced glucose was observable.

After several attempts to test the electrodes produced, it was not possible to produce results similar to those we used as a basis for comparison. We were able to verify very small current increases when the concentration of glucose in the sample being analyzed was much higher than the target concentration, in this case the range of glucose concentrations present in sweat (20 M - 1.79 mM).

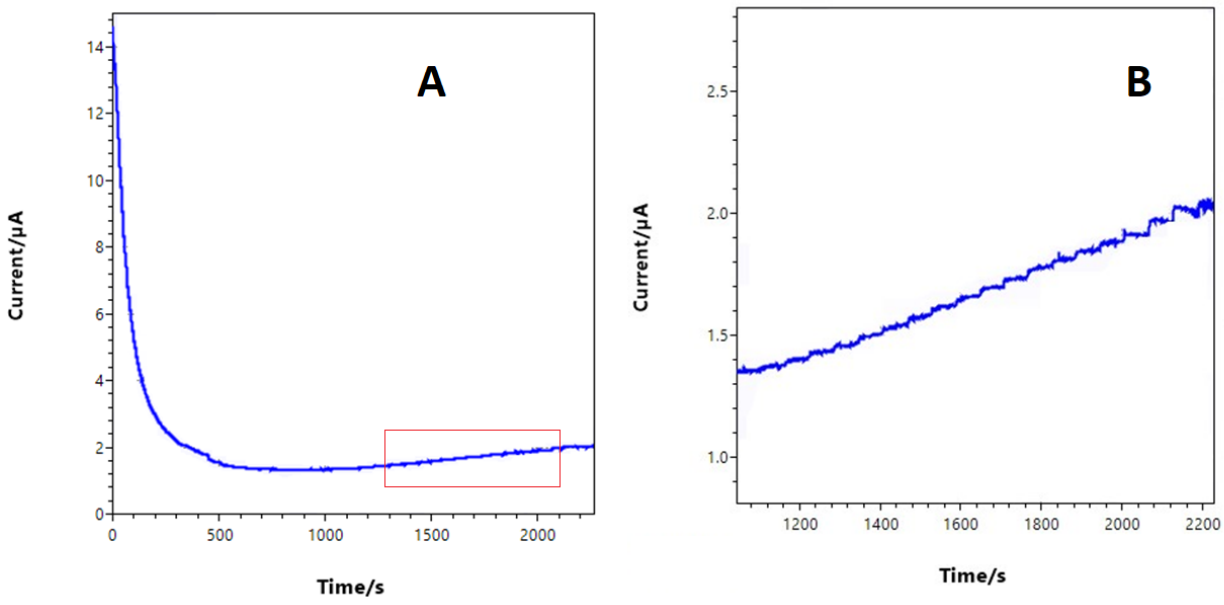

Figure 3.14 —Continuous amperometric sensor response to different glucose concentrations. (A) - P8S11 LIG/NiNPs biosensor, (B) - Same sample zoomed out. The chronoamperograms were obtained using the glucose sensor at 0.5 V. The inset shows the magnified section of amperograms for a time window of 1650 to 2200 seconds.

4.

Conclusions and Future Perspectives

The primary goal of this thesis was to create a biosensor for detecting glucose, utilizing LIG on a cost-effective and eco-friendly material such as paper. This sensor must be able to identify small levels of glucose by mimicking bodily fluids, such as sweat, to develop a non-intrusive method of testing.

The goals were not fully met as the sensor created did not respond to glucose as anticipated. Yet, it was achievable to develop a biosensor that had excellent electrochemical properties (CV results), all while being environmentally friendly, affordable, compact, and user-friendly.

Following sensor production, optimization occurred to determine the optimal LIG parameters (speed and power, P8S11), with P8S11 emerging as the top choice. Despite not displaying the lowest resistance value (18,24 Ω/sq), analysis of the LIG pattern and paper substrate confirmed paper fiber conversion into LIG and NiNP deposition in the LIG matrix, confirming compatibility with Direct Laser Writing on this substrate.

During this study, the biosensor's ability to operate as an electrochemical device was assessed using cyclic voltammetry and chronoamperometry as the primary electrochemical techniques.

An average CV with ferri-ferrocyanide redox probes demonstrated the effectiveness of the created sensor for such applications, allowing for potential adjustments to the working electrode.

Regarding the glucose tests, the bionsensor was able to detect glucose, however it was not able to detect it in the expected concentration range (sweat range 20 M - 1.79 mM).

Further investigation can be done to optimize the chemical treatment using different types and concentrations of nickel precursors, aiming to enhance selectivity in the sensor and achieve improved detection limits.

Finding new ways to integrate NiNPs into LIG would be beneficial, as it was a main focus in this study and did not meet expectations. While the biosensor did contain NiNPs and successfully detected glucose, increasing the quantity of NiNPs in a crystalline form (for XRD samples that identify NiO peaks) would, perhaps, enhance the electrode's response to glucose. Further studies and testing are needed to create a biosensor with better sensitivity, precision and greater ability to react to glucose.

5

BIBLIOGRAPHY

[1] S. A. and N. M. "A review of types 1 and 2 diabetes mellitus and their treatment with insulin". In: American Journal of Therapeutics 13.4 (2006), pp. 349–361. issn: 1075-2765.

[2] Y. Zhai, Z. Zhu, and S. Dong. "ChemInform Abstract: Carbon-Based Nanostructures for Advanced Catalysis". In: ChemInform 46.44 (2015), no–no. doi: 10.100 2/chin.20154427

[3] T. H. E. Royal, S. Academy, and O. F. Sciences. "compiled by the Class for Physics of the Royal Swedish Academy of Sciences Graphene". In: The Royal Swedish Academy of Sciences 50005.October (2010), pp. 0–10. issn: 1476-4687. arXiv: 1011.4680.

[4] X. J. Lee et al. "Review on graphene and its derivatives: Synthesis methods and potential industrial implementation". In: Journal of the Taiwan Institute of Chemical Engineers 98.xxxx (2019), pp. 163–180. issn: 18761070. doi: 10.1016 /j.jtice.2018.10.028.

[5] S. Chaitoglou, E. Bertran, and J. L. Andujar. "Growth Study and Characterization of Single-Layer Graphene Structures Deposited on Copper Substrate by Chemical Vapour Deposition". In: Graphene Materials - Structure, Properties and Modifications November (2017). doi: 10.5772/67439.

[6] R. Ye, D. K. James, and J. M. Tour, "Laser-Induced Graphene," Acc Chem Res, vol. 51, no. 7, pp. 1609–1620, Jul. 2018, doi: 10.1021/ACS.ACCOUNTS.8B00084.

[7] J. Kang, W. Cao, X. Xie, D. Sarkar, W. Liu, and K. Banerjee, "Graphene and beyond-graphene 2D crystals for next-generation green electronics," Micro- and Nanotechnology Sensors, Systems, and Applications VI, vol. 9083, p. 908305, Jun. 2014, doi: 10.1117/12.2051198.

[8] A. Kaidarova et al. "Wearable multifunctional printed graphene sensors". In: npj Flexible Electronics 3.1 (2019), pp. 1–10. issn: 23974621. doi: 10.1038/s41528-019-0061-5.

[9] M. G. Stanford et al. "Laser-Induced Graphene for Flexible and Embeddable Gas Sensors". In: ACS Nano 13.3 (2019), pp. 3474–3482. issn: 1936086X. doi: 10.1021/acsnano.8b09622.

[10] Y. Zhu et al. "Highly sensitive and skin-like pressure sensor based on asymmetric double-layered structures of reduced graphite oxide". In: Sensors and Actuators, B: Chemical 255 (2018), pp. 1262–1267. issn: 09254005. doi: 10.1016/j.snb.2017.08.116.

[11] A. Prabhakaran and P. Nayak. "Surface Engineering of Laser-Scribed Graphene Sensor Enables Non-Enzymatic Glucose Detection in Human Body Fluids". In: ACS Applied Nano Materials 3.1 (2020), pp. 391–398. issn: 25740970. doi: 10.1021/acsanm.9b02025.

[12] H. Yoon et al. "A chemically modified laser-induced porous graphene based flexible and ultrasensitive electrochemical biosensor for sweat glucose detection". In: Sensors and Actuators, B: Chemical 311 (2020), p. 127866. issn: 09254005. doi: 10.1016/j.snb.2020.127866.

[13] Y. Zhang et al. "A flexible non-enzymatic glucose sensor based on copper nanoparticles anchored on laser-induced graphene". In: Carbon 156 (2020), pp. 506–513. issn: 00086223. doi: 10.1016/j.carbon.2019.10.006.

[14] A. Behrent, C. Griesche, P. Sippel, and A. J. Baeumner, "Process-property correlations in laser-induced graphene electrodes for electrochemical sensing," Microchimica Acta, vol. 188, no. 5, pp. 1–14, May 2021, doi: 10.1007/S00604-021-04792-3/FIGURES/8.

[15] R. Ye, D. K. James, and J. M. Tour. "Laser-Induced Graphene: From Discovery to Translation". In: Advanced Materials 31.1 (2019), pp. 1–15. issn: 15214095. doi: 10.1002/adma.201803621.

[16] Y. Chyan et al. "Laser-Induced Graphene by Multiple Lasing: Toward Electronics on Cloth, Paper, and Food". In: ACS Nano 12.3 (2018), pp. 2176–2183. issn: 1936086X. doi: 10.1021/acsnano.7b08539.

[17] T. Pinheiro et al., "Laser-Induced Graphene on Paper toward Efficient Fabrication of Flexible, Planar Electrodes for Electrochemical Sensing," Adv Mater Interfaces, vol. 8, no. 22, pp. 1–12, 2021, doi: 10.1002/admi.202101502.

[18] A. Filipe and D. O. S. Santos, "Bachelor of Science SINGLE-STEP LASER-INDUCED GRAPHENE AS A PLATFORM FOR MONITORING PH WITHIN SMART BANDAGES FOR WOUND," 2022.

[19] J. C. Caetano, "DEPARTMENT OF PHYSICS DEVELOPMENT OF A LOW-COST, NON-ENZYMATIC GLUCOSE SENSOR BASED ON COPPER NANOPARTICLES AND LASER-INDUCED GRAPHENE TOWARDS WEARABLE SENSING," 2021.

[20] G. Bhattacharya et al., "Disposable Paper-Based Biosensors: Optimizing the Electrochemical Properties of Laser-Induced Graphene," ACS Appl. Mater. Interfaces, vol. 2022, p. 16, 3110, doi: 10.1021/acsami.2c06350.

[21] B. Kulyk, S. O. Pereira, A. J. S. Fernandes, E. Fortunato, F. M. Costa, and N. F. Santos, "Laser-induced graphene from paper for non-enzymatic uric acid electrochemical sensing in urine," Carbon N Y, vol. 197, pp. 253–263, Sep. 2022, doi: 10.1016/J.CARBON.2022.06.013.

[8] D. R. Thévenot, K. Toth, R. A. Durst, and G. S. Wilson, "Electrochemical biosensors: Recommended definitions and classification," Biosens Bioelectron, vol. 16, no. 1–2, pp. 121–131, 2001, doi: 10.1016/S0956-5663(01)00115-4.

[22] N. J. Ronkainen, H. B. Halsall, and W. R. Heineman, "Electrochemical biosensors," 2010, doi: 10.1039/b714449k.

[23] H. Teymourian, A. Barfidokht, and J. Wang. "Electrochemical glucose sensors

in diabetes management: An updated review (2010-2020)". In: Chemical Society Reviews 49.21 (2020), pp. 7671–7709. issn: 14604744. doi: 10.1039/d0cs00304b.

[24] C. Karunakaran, K. Bhargava, and R. Benjamin. Biosensors and Bioelectronics. Elsevier, 2015. isbn: 9780128031001. doi: 10.1016/C2014-0-03790-2.

[25] P. Zuman. Electrochemical Reactions and Mechanisms in Organic Chemistry. Vol. 73. 3. Elsevier, Dec. 2000, pp. 367–368. isbn: 9780444720078. doi: 10.1016/B978-0-444-72007-8.X5000-9.

[26] J. A. Rogers et al. "Optical Generation and Characterization of Acoustic Waves in Thin Films: Fundamentals and Applications". In: Annual Review of Materials Science 30.1 (Aug. 2000), pp. 117–157. issn: 0084-6600. doi: 10.1146/annurev.matsci.30.1.117.

[27] K. Honeychurch. "Printed thick-film biosensors". In: Printed Films. Elsevier, 2012, pp. 366–409. doi: 10.1533/9780857096210.2.366.

[28] A. C. Marques et al. Non-enzymatic lab-on-paper devices for biosensing applications. 1st ed. Vol. 89. Elsevier B.V., 2020, pp. 189–237. doi: 10.1016/bs.coac.2020.05.001.

[29] N. Shah, M. B. Arain, and M. Soylak. "Historical background: milestones in the field of development of analytical instrumentation". In: New Generation Green Solvents for Separation and Preconcentration of Organic and Inorganic Species (Jan. 2020), pp. 45–73. doi: 10.1016/B978-0-12-818569-8.00002-4.

[30] D. Harvey. Analytical Chemistry 2.1. 2016, p. 729.

[31] J. Heikenfeld et al. "Wearable sensors: Modalities, challenges, and prospects". In: Lab on a Chip 18.2 (2018), pp. 217–248. issn: 14730189. doi: 10.1039/c7lc009

[32] Yu, Yanan, et al. «Nickel Nanoparticle-Modified Electrode for Ultra-Sensitive Electrochemical Detection of Insulin». Biosensors and Bioelectronics, vol. 77, março de 2016, pp. 215–19. DOI.org (Crossref), https://doi.org/10.1016/j.bios.2015.09.036.

[33] Sabu, Chinnu, et al. «Advanced Biosensors for Glucose and Insulin». Biosensors and Bioelectronics, vol. 141, setembro de 2019, p. 111201. DOI.org (Crossref), https://doi.org/10.1016/j.bios.2019.03.034.

[34] Zhu, Jia, et al. «Laser-Induced Graphene Non-Enzymatic Glucose Sensors for on-Body Measurements». Biosensors and Bioelectronics, vol. 193, dezembro de 2021, p. 113606. DOI.org (Crossref), https://doi.org/10.1016/j.bios.2021.113606.

[35] Wang, Bo, et al. «Preparation of Nickel Nanoparticle/Graphene Composites for Non-Enzymatic Electrochemical Glucose Biosensor Applications». Materials Research Bulletin, vol. 49, janeiro de 2014, pp. 521–24. DOI.org (Crossref), https://doi.org/10.1016/j.materresbull.2013.08.066.

[36] D. Grieshaber, R. Mackenzie, J. Vörös, and E. Reimhult, "Electrochemical Biosensors-Sensor Principles and Architectures," Sensors, vol. 8, pp. 1400–1458, 2008, [Online]. Available: www.mdpi.org/sensors

[37] M. Pohanka, P. Skládal, and J. Appl Biomed, "Electrochemical Biosensors-Principles and Applications New analytical devices based on upconversion nanoparticles (UCNPs) View project Plasma polymers for immobilization of biomolecules and development of efficient immunosensors View project Journal of APPLIED BIOMEDICINE Electrochemical biosensors-principles and applications," Article in Journal of Applied Biomedicine, 2008, doi: 10.32725/jab.2008.008.

[38] A. Kudelski, "Analytical applications of Raman spectroscopy," Talanta, vol. 76, no. 1, pp. 1–8, Jun. 2008, doi: 10.1016/J.TALANTA.2008.02.042.

[39] H. Park, M. Kim, B. G. Kim, and Y. H. Kim, "Electronic Functionality Encoded Laser-Induced Graphene for Paper Electronics," Cite This: ACS Appl. Nano Mater, vol. 2020, pp. 6899–6904, 2020, doi: 10.1021/acsanm.0c01255.

[40] B. Kulyk et al., "Laser-Induced Graphene from Paper for Mechanical Sensing," Cite This: ACS Appl. Mater. Interfaces, vol. 13, pp. 10210–10221, 2021, doi: 10.1021/acsami.0c20270.

[41] A. Samouco, A. C. Marques, A. Pimentel, R. Martins, and E. Fortunato, "Laser-induced electrodes towards low-cost flexible UV ZnO sensors," Flexible and Printed Electronics, vol. 3, no. 4, p. 044002, Dec. 2018, doi: 10.1088/2058-8585/AAED77.

[42] M. Henini, "Scanning electron microscopy: an introduction," III-Vs Review, vol. 13, no. 4, pp. 40–44, Jul. 2000, doi: 10.1016/S0961-1290(00)80006-X.

[43] J. F. Rusling and S. L. Suib, "Characterizing Materials with Cyclic Voltammetry **."

[44] D. H. Evans, K. M. O'connell, R. A. Petersen, and M. J. Kelly, "Cyclic Voltammetry POTENTIAL, VOLTS," UTC, 2022. [Online]. Available: https://pubs.acs.org/sharingguidelines

[45] Leppäniemi, Jaakko, et al. «Far-UV Annealed Inkjet-Printed In 2 O 3 Semiconductor Layers for Thin-Film Transistors on a Flexible Polyethylene Naphthalate Substrate». ACS Applied Materials & Interfaces, vol. 9, n.o 10, março de 2017, pp. 8774–82. DOI.org (Crossref), https://doi.org/10.1021/acsami.6b14654.

[46] Carlos, Emanuel, et al. «Solution Combustion Synthesis: Towards a Sustainable Approach for Metal Oxides». Chemistry – A European Journal, vol. 26, n.o 42, julho de 2020, pp. 9099–125. DOI.org (Crossref), https://doi.org/10.1002/chem.202000678.

[47] Yin, Jun, et al. «Flexible 3D Porous Graphene Film Decorated with Nickel Nanoparticles for Absorption-Dominated Electromagnetic Interference Shielding». Chemical Engineering Journal, vol. 421, outubro de 2021, p. 129763. DOI.org (Crossref), https://doi.org/10.1016/j.cej.2021.129763.

[48] Y. Wang, Y.M. Li, L.H. Tang, J. Lu, J.H. Li, Electrochem. Commun. 11 (2009) 889–892.

[49] A.C. Ferrari, J. Robertson, Phys. Rev. B 61 (2000) 14095–14107.

[50] R. Martins, I. Ferreira, and E. Fortunato, "Electronics with and on paper," physica status solidi (RRL) – Rapid Research Letters, vol. 5, no. 9, pp. 332–335, Sep. 2011, doi: 10.1002/PSSR.201105247

[51] Pinheiro, T., Morais, M., Silvestre, S., Carlos, E., Coelho, J., Almeida, H. V., Barquinha, P., Fortunato, E., & Martins, R. (2024). Direct laser writing: from materials synthesis and conversion to electronic device processing. Advanced Materials. https://doi.org/10.1002/adma.202402014

[52] D. A. C. Brownson and C. E. Banks, “The Handbook of Graphene Electrochemistry,” The Handbook of Graphene Electrochemistry, pp. 1–201, Jan. 2014, doi: 10.1007/978-1 4471-6428-9/COVER.

A

APPENDIX

A.1 Tables and Images

5 Layers of Wax		
	Value (Ω/sq)	Standard Deviation
P6S6	12,38	1,09
P6S7	16,58	0,399
P6S9	25,51	1,24
P7S8	11,78	1,91
P7S9	14,97	0,741
P7S10	19,59	1,66
P8S9	12,34	2,19
P8S10	14,69	2,93
P8S11	18,24	1.50

Table A1 — Sheet resistance results for the chosen Laser conditions for 1 Laser Passing

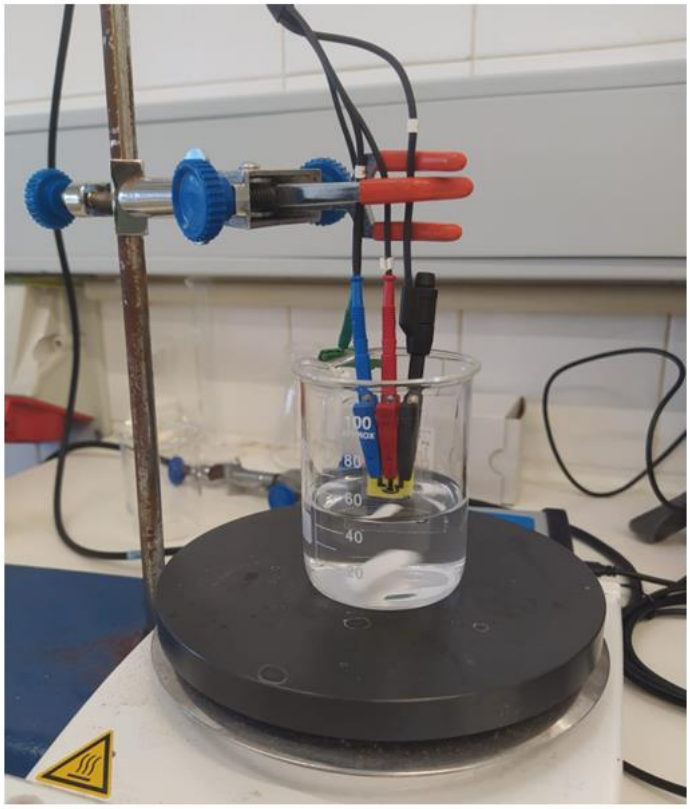

Figure A1 — Experimental setup used to perform glucose sensor tests. Retrieved from [19].